Active and Passive Elec. Comp., September 2003, Vol. 26, pp. 171–183

PREPARATION, CHARACTERIZATION AND ELECTROCHEMICAL LITHIUM INSERTION INTO THE NEW ORGANIC–INORGANIC POLY(3,4-ETHYLENE DIOXYTHIOPHENE)/V_2O_5 HYBRID

CHAI-WON KWON[a], A. VADIVEL MURUGAN[b] and GUY CAMPET[a,*]

[a]Institut de Chimie de la Matiére Condensèe de Bordeaux du CNRS, 87 Avenue du Dr. A. Schweitzer, 33608 Pessac Cedex, France; [b]Centre for Materials for Electronics Technology, Ministry of Communication and Information Technology, Govt. of India, Panchawati, Off-Pashan Road, Pune 411008, India

(Received 31 August 2002; In final form 17 November 2002)

Poly(3,4-ethylene dioxythiophene) (PEDOT) has been inserted between the layers of crystalline V_2O_5 via the in situ polymerization of EDOT within the framework of the oxyde. The insertion increases the bidimensionality of the V_2O_5 host by the layer separation but results in a random layer stacking structure, leading to broadening of the energy state distribution. According to electrochemical measurements, the hybrids showed reversible specific capacities up to ~330 mAh/g at 15 mA/g between 2 and 4.4 V vs. Li^+/Li.

Keywords: Poly(3,4-ethylene dioxythiophene); Vanadium oxide; Organo–inorganic hybrid

1 INTRODUCTION

Recent progress in 'nano-chemistry' gives birth to a new emerging area, so-called 'hybrid' or 'nanocomposite', which is a challenge for combining the properties of two or more different species into a unique material [1–4]. Especially in the field of lithium battery application, conducting polymer/V_2O_5 hybrids have received considerable attention over the past several years to profitably integrate many desirable properties of the vanadium oxide and of the polymeric counterpart [5–12]. V_2O_5 is one of the most beneficial lithium cathodes with processibility and high capacity, whereas conducting polymers have advantages including flexibility and conductivity. In addition, from an academic point of view, there are many interesting things to be investigated, such as the oxidation state of the vanadium, the doping character of the polymer and the nature of interaction between the polymer and the vanadium oxide. These hybrids are generally prepared by mixing V_2O_5 gel with monomers of the corresponding conducting polymer such as polyaniline (PANI), polypyrrole (PPY) or

* Corresponding author. E-mail: campet@icmcb.u-bordeaux.fr

ISSN 0882-7516 print; ISSN 1563-5031 online
DOI: 10.1080/1042015031000073904

polythiophene (PTH) [5–15]. The chemical structure of some selected conducting polymers is shown in Figure 1.

Among them, the PANI/V_2O_5 xerogel system is the most intensively studied [5, 6, 10–15]. The reaction between aniline and V_2O_5 xerogel proceeds via oxidative intercalation and subsequent polymerization of the aniline monomer concomitant with the reduction of V^{5+} to V^{4+} in the xerogel host. Kanatzidis and collaborators found that the growth of the polymer goes on mainly within the interlamellar space with the consumption of molecular oxygen [15]. Aging in air causes both partial reoxidation of the inorganic host, that is auto-recovery of V^{5+} from V^{4+}, and the post-polymerization of the organic intercalate. In this context, it is not surprising that the electrochemical performance of the PANI/V_2O_5 xerogel hybrid was found to be improved by a mild oxygen treatment. Leroux et al. could augment the lithium capacity of $PANI_{0.40}V_2O_5$ from 0.85 F/mol to 1.35 F/mol at ~10 mA/g after oxygen treatment at 150 °C for 8 h [5, 6]. They assigned this increase to the regeneration of ~2.9 V sites of the V_2O_5 host due to the recovery of V^{5+}. Lira-Cantú et al. optimized the oxygen treatment condition and reported that the thermal treatment under oxygen over 80 °C for more than 5 hrs may destroy the polymer chain [10–12]. Under optimized conditions, 302 mAh/g (2.72 F/mol) at ~C/48 could be achieved. This enhancement is attributed to the evasion of the degradation of the polymer chain, leading to the formation of new ~2.3 V-sites probably related to the polymer.

On the contrary, hybrid systems based on PPY/V_2O_5 or PTH/V_2O_5 are relatively less studied. The position of the heteroatom makes the distinction in chemistry and physico-chemical properties between PANI on one side and PPY or PTH on the other side [16]. The N atom of PANI is outside the ring and participates directly in the polymerization process, whereas the heteroatom N or S for PPY or PTH, respectively, is one of the ring component members and, instead, the alpha carbon takes part in the polymer linkage. Concerning PPY/V_2O_5 hybrids, it was reported that only a partial reoxidation was attained even after 72 h O_2 exposure at 150 °C, and moreover the capacity decreased owing to the polymer degradation [6, 7]. On the other hand, the hybrids prepared under reflux conditions have fully oxidized vanadium, and show an improved performance. To $PPY_{0.40}V_2O_5$ prepared under reflux conditions, about 1.8 Li/mol could be inserted at ~10 mA/g.

As for the PTH/V_2O_5 hybrids, the thiophene monomer is not easy to insert directly into V_2O_5, because thiophene has a greater redox potential (~3.8 V vs. Li^+/Li) than that of V_2O_5 (~3.4 V vs. Li^+/Li). Goward et al. made several types of the PTH/V_2O_5 hybrids with bithiophene, terthiophene, 3-methyl thiophene and 2,5-methyl thiophene, and examined their

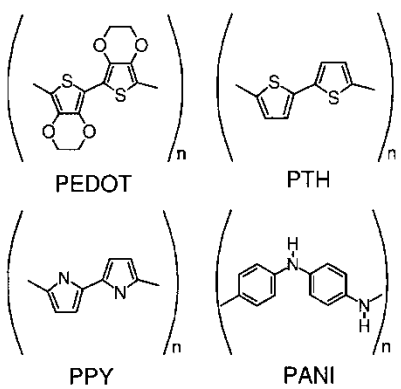

FIGURE 1 Chemical structure of some selected conductive polymers: PEDOT (poly(3,4-ethylene dioxythiophene)), PTH (polythiophene), PPY (polypyrrole) and PANI (polyaniline).

electrochemical properties [7]. Regarding 3-methyl thiophene, the methylation in the 3-position facilitates α–α' coupling and thereupon more regular structure, whereas in the case of 2,5-dimethyl thiophene, α–β' or/and β–β' coupling deteriorates polymeric order, leading to a decrease in the electrochemical capacity. The hybrids made from terthiophene and 3-methyl thiophene exhibit a better capacity of $\sim$0.95 Li/mol at 10 mA/g than those from bithiophene ($\sim$0.70 Li/mol) and from 2,5-dimethyl thiophene ($\sim$0.58 Li/mol). The hybrids seem to be sensitive to both polymer nature and overall order in the material. In this standpoint, PEDOT is expected to form a hybrid system with better electrochemical properties, as its cap in 3 and 4 positions with the ethylenedioxy group will lead to a more regular polymeric order [16, 17].

We have currently succeeded in the preparation of a new series of PEDOT/V_2O_5 [18–20]. To our knowledge, this is the first conducting polymer/V_2O_5 hybrid system synthesized starting with well-crystalline vanadium oxide. Furthermore, the PEDOT is probably the conducting polymer of choice, as it has been reported to exhibit excellent electrical conductivity up to 550 S cm^{-1} with air-stability superior to PANI, PPY and PTH [16, 17, 21]. We observed that these hybrids showed enhanced electrochemical capacities and that their lithium insertion behaviors were not similar to those of crystalline V_2O_5 but to those of other hybrid systems based on V_2O_5 gel. Here we will describe a systematic study of preparation, characterization and electrochemical lithium insertion into the hybrids.

2 EXPERIMENTAL SECTION

2.1 Materials

Vanadium pentoxide (99.9%), lithium metal foil (99.9%), $LiClO_4$ (99.99%), polytetrafluoroethylene (PTFE, 99.99%), propylene carbonate (PC, 99.9%) and dimethyl carbonate (DMC, 99%) from Aldrich were used without further purification. 3,4-ethylene dioxythiophene (EDOT, Bayer AG Germany) was distilled under vacuum prior to use. Ethylene carbonate (EC, Prolabo 99%) and ketjenblack were used as received. All the experiments were conducted with deionized water.

2.2 Sample Preparation

The PEDOT/V_2O_5 hybrids were synthesized by insertion and subsequent polymerization of EDOT into V_2O_5. A given amount of EDOT was dissolved in 25 ml of distilled water, and this solution was mixed and refluxed with 2 g of vanadium pentoxide for 12 h. The nominal molar ratio of EDOT to V_2O_5 was adjusted to 0.02 (VP1), 0.04 (VP2), 0.08 (VP3), 0.40 (VP4) or 0.60 (VP5). After completion of the reaction, the solid was filtered off and washed repeatedly with water and acetone until the initial light yellow color in the filtrate disappeared totally, and the resulting bluish-black powder was dried in air.

For comparison, Cl^- doped PEDOT was also prepared as reported in [21]. A given amount of EDOT was added in $FeCl_3$ aqueous solution at a molar ratio of $FeCl_3$:EDOT = 2.5:1, and stirred over 24 hours.

2.3 Physico-chemical Characterization

The incorporation of the polymer into the V_2O_5 was confirmed by powder-XRD spectra recorded with a Phillips PW-1050 X-ray diffractometer using Ni-filtered Cu-Kα radiation ($\lambda = 1.5418$ Å). Fourier transform infrared (FTIR) spectra of powder samples diluted with

KBr were recorded with a Bruker FTIR spectrometer in transmission mode. The variation of particle morphology upon the intercalation was monitored by a scanning electron micrograph (SEM, Philips XL-30) or by a transmission electron microscope (TEM, JEOL 2000 FX) operating at an accelerating voltage of 200 kV. The molar fraction of polymer per V_2O_5 was determined by thermal analysis with a Shimadzu TGA-50 system from room temperature to 800 °C at a rate of 10 °C/min under oxygen. Electrical conductivity was measured by a conventional four-probe method using conducting silver paint for contacts. Elemental analysis was carried out using inductively coupled plasma optical emission spectroscopy (ICP-OES, Perkin-Elmer 1000) and E-Instruments-EA 1110 CHNS-O Analyser.

2.4 Electrochemistry

The electrochemical measurements were performed using button-type two-electrode cells with the aid of a computer-controlled PGS201T (Tacussel) potentiostat/galvanostat system. The composite cathodes were made by intimately mixing 70% (by mass) of the active material, 25% of Ketjenblack and 5% of PTFE. The surface area of electrodes and the mass of active material were adjusted to ~1 cm^2 and ~20 mg, respectively, for reproducibility. These electrodes were dried under vacuum at ~80 °C for more than 3 hours, and introduced into an Argon-filled glove box without any exposure to air. The electrolyte was a 1 M solution of $LiClO_4$ in a 1:1 mixture (by volume) of EC/DMC. Lithium foil was used as an anode.

3 BASIC CHARACTERIZATION OF PEDOT/V_2O_5 HYBRIDS

3.1 Determination of Chemical Composition

As already well known in the field of intercalation chemistry, all the guest reactant would not always be intercalated into the host. The determination of the chemical composition of the intercalation compounds is important for this reason. The chemical composition of the PEDOT/V_2O_5 hybrid samples was estimated from ICP, CHNS and thermal analysis (Tab. I). Figure 2 presents the thermogravimetry (TG) and differential scanning calorimetry (DSC) curves of the VP3 sample as a representative. The TG curves can be divided into three temperature domains of 25–130, 130–420 and 420–650 °C.

The first step up to 130 °C is attributed to removal of water, confirmed by the endothermic peak of the DSC curve. Next weight loss until 420 °C is due to the combustion of the polymer component, which corresponds well to the exothermic DSC peak. The abrupt weight loss around 210 °C is assigned to the decomposition of the ethylenedioxy groups of the polymer. A mass gain to 650 °C is ascribed to the endothermic oxygen uptake, which occurs together with the conversion of V^{4+} into V^{5+} [6]. This result proposes that the insertion and polymer-

TABLE I Results of ICP and CHNS Elemental Analysis.

	Nominal EDOT/V_2O_5 ratio	C/V atomic ratio	S/V atomic ratio
VP1	0.02	0.08	0.00606
VP2	0.04	0.129	0.0102
VP3	0.08	0.202	0.0442
VP4	0.40	0.659	0.174
VP5	0.60	0.858	0.229

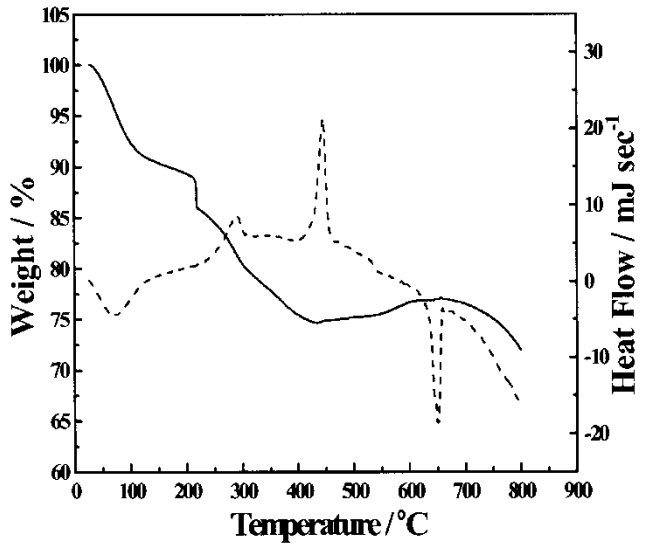

FIGURE 2 Thermogravimetry (solid line) and differential scanning calorimetry (dashed line) curves for VP3 sample as a representive.

ization of the EDOT monomer is accompanied by a 'sacrificial' reduction of the V_2O_5 layers. Based on the results of elemental and thermal analysis, the formulas of the hybrids are evaluated and listed in Table II.

3.2 X-ray Diffraction Study

The change of crystal structure upon the incorporation of the polymer into V_2O_5 was monitored by powder X-ray diffraction. Series of well-developed (0 0 1) peaks can be observed, and the d-spacing increases from 4.3 Å to 13.8 Å and further to 19.0 Å depending on the amount of the incorporated macromolecules (Fig. 3). The net interlayer expansion increases from 5.1 Å for VP1 to 10.3 Å for VP5, assuming the V_2O_5 slab is composed of two vanadium oxide sheets like that of vanadium oxide xerogel [22, 23]. This would indicate that the expansion proceeds in two steps, first forming a monolayer of polymer and then double layers (Fig. 4). It is noted that (h k 0) reflections of the hybrids correspond to those of the pristine V_2O_5 and that some of them, such as (1 1 0) and (3 1 0), show a diffuse peak shape, rising rather rapidly and then declining slowly towards the high angle side. This feature suggests that the compounds have a random layer stacking structure, which

TABLE II Nominal EDOT/V_2O_5 Ratio and Corresponding Chemical Composition for the Hybrid Samples.

	Nominal EDOT/V_2O_5 ratio	Output/Input ratio	Chemical composition*
VP1	0.02	1	$(C_6H_4O_2S)_{0.02}V_2O_{4.9}$
VP2	0.04	0.75	$(C_6H_4O_2S)_{0.03}V_2O_{4.8}$
VP3	0.08	0.625	$(C_6H_4O_2S)_{0.05}V_2O_{4.7}$
VP4	0.40	0.45	$(C_6H_4O_2S)_{0.18}V_2O_{4.6}$
VP5	0.60	0.42	$(C_6H_4O_2S)_{0.25}V_2O_{4.6}$

*The surface-adsorbed water contents are ignored.

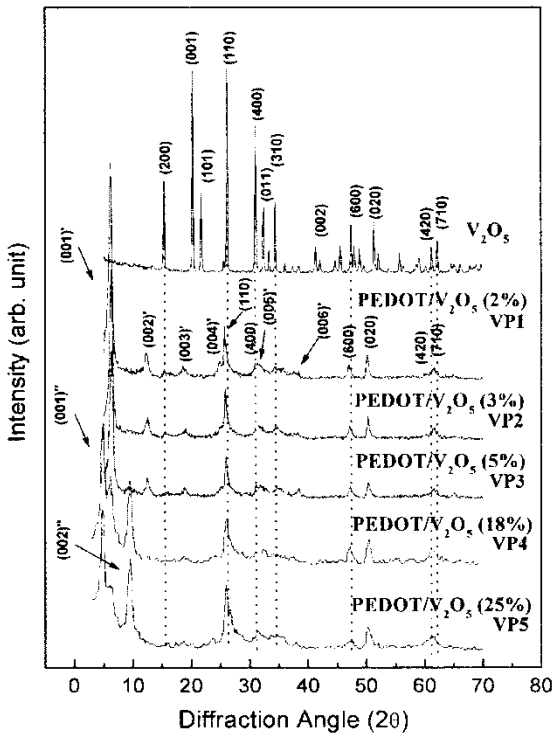

FIGURE 3 Powder X-ray diffraction patterns of pristine V_2O_5, VP1, VP2, VP3, VP4 and VP5.

consists of equidistant and parallel (a–b) layers, but randomly rotated about the normal c-axis [24]. Such characteristics have already been found for V_2O_5 compounds prepared by electrolysis or ozone-oxidation of $VOSO_4$ or by the reaction of metallic vanadium and hydrogen peroxide [25–29]. These V_2O_5 compounds have so-called 'bidimensional' structure, which is stabilized by interlayer water molecules. Such structural characteristics would be similar to those of PEDOT/V_2O_5 hybrids, except the replacement of water molecules by

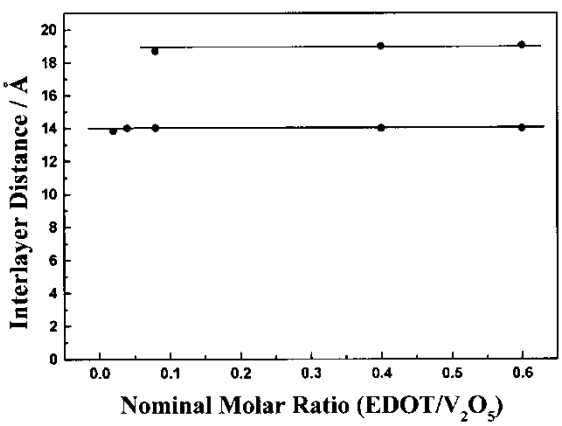

FIGURE 4 Evolution of interlayer distance upon increasing nominal molar ratio of EDOT to V_2O_5.

TABLE III Nominal EDOT/V_2O_5 Ratio, Corresponding Chemical Composition and d-spacing for the Pristine V_2O_5 and Hybrid Samples.

	Nominal EDOT/V_2O_5 ratio	Chemical composition	d-spacing (Å)
V_2O_5	–	V_2O_5	4.37*
VP1	0.02	$(C_6H_4O_2S)_{0.02}V_2O_{4.9}$	13.8
VP2	0.04	$(C_6H_4O_2S)_{0.03}V_2O_{4.8}$	14.0
VP3	0.08	$(C_6H_4O_2S)_{0.05}V_2O_{4.7}$	14.0
VP4	0.40	$(C_6H_4O_2S)_{0.18}V_2O_{4.6}$	17.8
VP5	0.60	$(C_6H_4O_2S)_{0.25}V_2O_{4.6}$	19.0

*If two slabs of layer is taken as a block, the d-spacing would be ~8.7 Å Refs. [22, 23].

hydrophobic polymer chains. For simplicity and clarity, these kinds of V_2O_5 will be denoted as 2D-V_2O_5 below.

The details are summarized in Table III with the results of elemental analysis.

3.3 Infrared Spectroscopy

In order to examine the oxidation state of vanadium and the doping state of the polymer, Fourier transform infrared (FTIR) spectra were recorded. The spectra of the hybrids shown in Figure 5 display the characteristic bands corresponding to both PEDOT and V_2O_5. Vibrations around 1520, 1450 and 1380 cm^{-1} are assigned to the stretching of C═C and C—C in the thiophene ring, and those at 1130 and 1090 cm^{-1} to the stretching of the ethylenedioxy group (Fig. 5(a)) [30–36]. These peaks increase as the amount of incorporated polymer augments, which proves the presence of the PEDOT in these materials. The absence of peaks at 1490 and 1190 cm^{-1} implies that the organics are not in monomer form but in polymeric form. The peaks around 1260 and 1090 cm^{-1} indicate that the polymer is in doped state, leading to an increased conductivity [31, 36]. The changes in the position and shape of the vibrational peaks of the vanadium oxide framework are also significant.

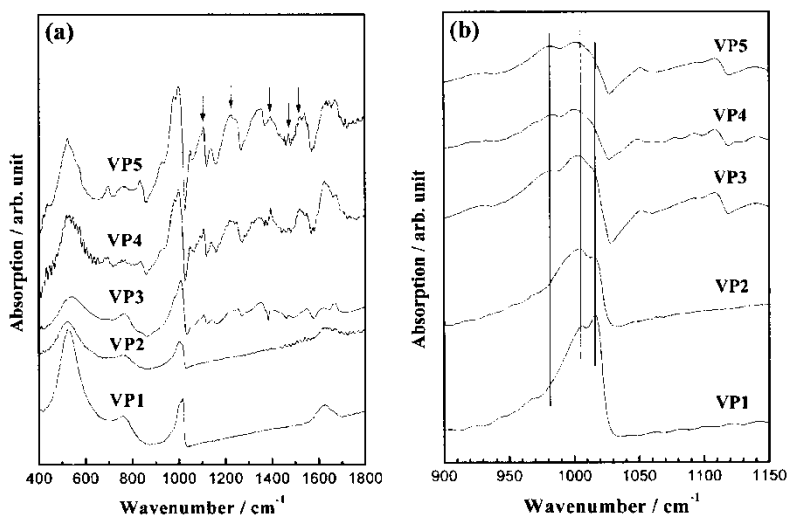

FIGURE 5 Infrared spectra for VP1, VP2, VP3, VP4 and VP5 in the range of (a) 400–1800 cm^{-1} and (b) 900–1150 cm^{-1} (enlargement). The samples were diluted with KBr and pressed into a pellet. Some important peaks from the polymer are marked with arrows.

Bands around 530 and 810 cm^{-1} are attributed to V—O—V stretching modes and those around 1000 cm^{-1} to V═O stretching. Compared with well-crystalline V_2O_5, the V═O peak shifts from 990 to 1000 cm^{-1} and the V—O—V vibrational peaks shift from 850 and 550 cm^{-1} to 810 and 530 cm^{-1}, respectively, accounting for the greater number of V^{4+} centers in the hybrids. The mechanism of this remarkable all-solid-state intra-lamellar polymerization is presumed to be coupled to the ability of vanadium centers to activate oxygen which is the primary electron acceptor in this process. Therefore, vanadium oxide plays a direct role in this redox event, which is consistent with its ability to catalyze several oxidation

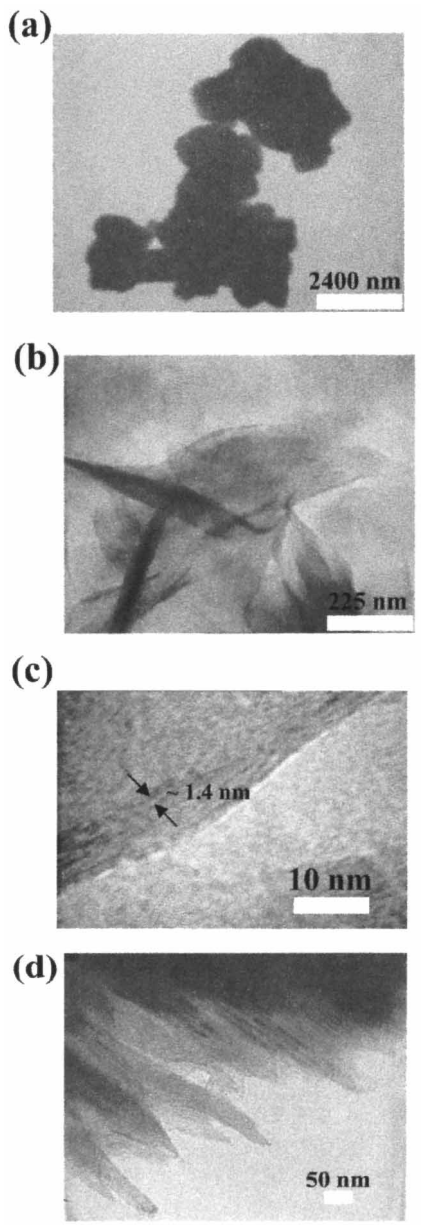

FIGURE 6 Transmission electron micrographs for (a) pristine V_2O_5, (b) and (c) VP1, and (d) VP5.

reactions of organic molecules [37]. A deeper inspection finds that the $985\,cm^{-1}$ peak increases and the $1015\,cm^{-1}$ peak decreases inversely as the amount of incorporated polymer augments (Fig. 5(b)), which suggests a strong interaction (e.g. hydrogen bonding) between the vanadyl group and the incorporated polymer, like PPY/V_2O_5 xerogel hybrid [8].

3.4 Electron Microscopy

The influence of this modification on particle morphology was observed with scanning and transmission electron microscopy. The $PEDOT/V_2O_5$ hybrid forms a continuous and relatively homogeneous matrix with a clean lamellar surface, which evidences the incorporation of PEDOT into the V_2O_5 in agreement with the results of XRD patterns. More importantly, the SEM micrographs also suggest that there is no bulk deposition of polymer alone between the micro-crystallites. A deeper observation of particle morphology was realized using transmission electron microscopy. The pristine V_2O_5 consists of thick agglomerated particles with irregular sizes of micrometer order (Fig. 6(a)), whereas the particles of hybrids are composed of well-developed (a–b) planes stacked along with c-axis (Fig. 6(b)–(d)). The stacking length in the c-direction is much shorter compared with a and b directions for the hybrids, which would be considered as the enhancement of 'bidimensionality'. The interlayer spacing of VP1 has been estimated by measuring the length from one dark line to the nearest one, which gives $\sim 14\,Å$ in good agreement with the XRD result.

3.5 Electrical Conductivity

The electrical transport behaviors of the hybrids could be understood by considering the insertion of PEDOT into V_2O_5 powder as a hybrid system where two different types of low-dimensional electronic conductors coexist at the molecular level in a dimensionally constrained environment. Two types of charge carriers may be present in these materials, small polarons (electrons) associated with the $d^1(V^{4+})$ centers on the vanadium oxide lattice, and large polarons on the PEDOT backbone. The actual nature of the charge transport would depend on the relative mobility of these two different kinds of carriers as demonstrated by the fact that the electronic conductivity of $PEDOT/V_2O_5$ hybrids is up to four orders of magnitude higher than that of pristine V_2O_5. In all samples, the conductivity increases with rising temperature as has been observed in most intercalated compounds and conjugated polymers [15, 38]. The conductivity raises from 10^{-5} to $10^{-1}\,S\,cm^{-1}$ as the amount of incorporated polymer augments from VP1 to VP5, although the exact mechanism may be more complex due to the smaller particle size contribution towards grain conductivity. In this case, however, the increase in conductivity is probably due to a continued process of growth of the organic polymer network. The detailed results are summarized in Table IV.

TABLE IV Nominal $EDOT/V_2O_5$ Ratio, Chemical Compositions, d-spacing and Electrical Conductivity for the Pristine V_2O_5 and Hybrids.

	Nominal EDOT/V_2O_5 ratio	Chemical composition	d-spacing (Å)	Conductivity ($S\,cm^{-1}$)
V_2O_5	–	V_2O_5	4.3	8.78×10^{-5}
VP1	0.02	$(C_6H_4O_2S)_{0.02}V_2O_{4.9}$	13.8	2.92×10^{-3}
VP2	0.04	$(C_6H_4O_2S)_{0.03}V_2O_{4.8}$	14.0	6.97×10^{-3}
VP3	0.08	$(C_6H_4O_2S)_{0.05}V_2O_{4.7}$	14.0	3.84×10^{-2}
VP4	0.40	$(C_6H_4O_2S)_{0.18}V_2O_{4.6}$	17.8	9.82×10^{-2}
VP5	0.60	$(C_6H_4O_2S)_{0.25}V_2O_{4.6}$	19.0	1.01×10^{-1}

4 ELECTROCHEMISTRY

Vanadium oxide host lattice has been considered as one of the best cathode materials in secondary Li-batteries, mainly due to its layered structure immensely suitable for Li-insertion [39–41]. For battery applications, the rate-limiting step is reported to be the reduction of V_2O_5 material during discharge accompanied by Li^+ insertion [42]. One common strategy to achieve higher efficiency and lithium uptake is to use high surface area materials, so that the distance over which Li^+ must diffuse through the host material is minimized [40, 41]. In this case, an innegligible amount of Li can be reversibly grafted on large surface materials. Another approach that has not been completely explored yet, is to manipulate the interlayer spacing in these layered materials by using various intercalants so as to enhance the rate of Li^+ migration, since intercalation generally leads to changes in the interlayer spacing for layered materials [43, 44]. Examples of such intercalants include pyrrole and aniline, all of which are known to oxidatively polymerize when intercalated into highly oxidizing materials such as V_2O_5 [6–8]. The electrochemical insertion of Li in V_2O_5 material can be described by the following redox reaction.

$$xLi^+ + xe^- + V_2O_5 \leftrightarrow Li_xV_2O_5.$$

For PEDOT/V_2O_5 hybrids, analogous electrochemical reactions would be applicable as follows.

(Reduction of PEDOT)

$$[PEDOT^+]_xV_2O_5^{x-} + xLi^+ + xe^- \leftrightarrow Li_x[PEDOT]_xV_2O_5^{x-}.$$

(Reduction of $V_2O_5^{x-}$)

$$Li_x[PEDOT]_xV_2O_5^{x-} + yLi^+ + ye^- \leftrightarrow Li_{x+y}[PEDOT]_xV_2O_5^{-(x+y)}.$$

The open-circuit voltage (OCV) of the composites versus lithium metal anode is found to vary depending on the PEDOT/V_2O_5 ratio and obviously all hybrids give higher OCV values (3.77–3.61 V) than that observed (3.43 V) for pure V_2O_5 (Tab. V). This can be explained by two factors. One is that the electrochemical potential for incorporated PEDOT (∼3.8 V vs. Li^+/Li) is higher than that of V_2O_5 (∼3.4 V vs. Li^+/Li), and consequently all the hybrids exhibit higher OCV than pristine V_2O_5. The other factor is that the increased amount of incorporated polymer gives an augmented number of V^{4+} centers, as observed in the IR spectra, and thereby among the hybrid samples, the monolayer-incorporated hybrids (VP1, VP2 and VP3) deliver higher OCV than the double layer-incorporated ones (VP4 and VP5).

TABLE V Nominal EDOT/V_2O_5 Ratio, Corresponding Chemical Composition and Open Circuit Voltage vs. Li^+/Li for the Pristine V_2O_5 and Hybrid Samples.

	Nominal EDOT/V_2O_5 ratio	Chemical composition	Open circuit voltage (V)
V_2O_5	–	V_2O_5	3.43
VP1	0.02	$(C_6H_4O_2S)_{0.02}V_2O_{4.9}$	3.74
VP2	0.04	$(C_6H_4O_2S)_{0.03}V_2O_{4.8}$	3.76
VP3	0.08	$(C_6H_4O_2S)_{0.05}V_2O_{4.7}$	3.77
VP4	0.40	$(C_6H_4O_2S)_{0.18}V_2O_{4.6}$	3.62
VP5	0.60	$(C_6H_4O_2S)_{0.25}V_2O_{4.6}$	3.61

An accurate inspection of insertion voltage is accomplished by analysis of the differential capacity profiles of the first discharges (Fig. 7). The sharp peaks of pristine V_2O_5 are typical traits of the phase transformations, while on the contrary the hybrids exhibit broad peaks, which would sustain our above argumentation on the sub-bandgap states. VP1 shows three peaks at 2.9, 2.5 and 2.3 V analogous to PPY/V_2O_5 and PANI/V_2O_5 hybrids [5–7, 10, 11]. In the case of PANI/V_2O_5 hybrids, the 2.3 V peaks could be increased after appropriate oxygen treatment, which was attributed to the polymer [10, 11]. But in our case, the hybrids also display 2.3 V peak although PEDOT has no redox capacity around 2.3 V. We therefore suggest the possibility that the origin of the 2.3 V capacity might come from the synergetic interaction between V_2O_5 layers and polymer chains, not from the polymers alone. For VP5, the 2.9 V peak shift down to 2.7 V, and the 2.3 V peak is less obvious, which also supports this idea. Consequently, the origin of the 2.3 V peak needs to be treated with special care for further studies.

In order to clarify the role of the polymer incorporation on the electrochemical performance for extended cycling, the variation of discharge capacities were measured on VP1 and VP5 as a representative for monolayer and double-layer incorporated systems, respectively (Fig. 8). VP1 maintains capacities over 300 mAh/g for ten cycles. All the hybrids provide larger capacity and better cyclability than the pristine V_2O_5. The improved performances are presumably due to a higher electrical conductivity and to the separation between vanadium oxide layers, leading to an enhanced bidimensionality.

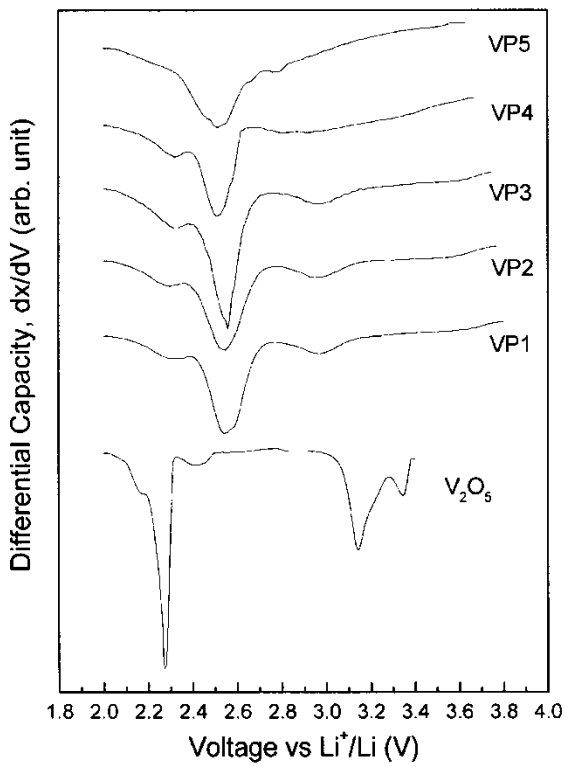

FIGURE 7 The first differential capacity profiles of the first discharges of the pristine V_2O_5 and hybrids.

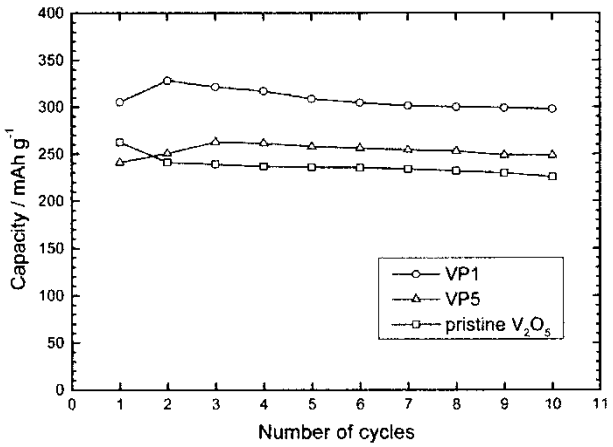

FIGURE 8 Evolution of discharge capacity with the number of cycles for pristine V_2O_5, VP1 and VP5. The data were obtained at a current density of 15 mA/g. The potential range was set to 2.0–4.2 V vs. Li for V_2O_5, and to 2.0–4.4 V for VP1 and VP5.

5 CONCLUSION

We have found a novel method of inserting PEDOT between the layers of V_2O_5 using a soft process of intercalation. The reaction takes place with the in situ polymerization of EDOT within the framework of crystalline V_2O_5 with different nominal EDOT/V_2O_5 ratios. XRD experiments prove the interlayer distance of V_2O_5 expands upon the incorporation of polymer step-by-step, first forming a monolayer and then double layers depending on the amount of incorporated polymer. The insertion reaction results in a random layer stacking structure, leading to broadening of the energy state distribution. IR spectra suggest the occurrence of V^{4+} centers upon the insertion reaction and a strong interaction between the vanadyl group and the incorporated polymer. From the electron microscopy results, it has been found that the incorporation of PEDOT increases the bidimensionality of the V_2O_5 host by the layer separation. According to electrochemical measurements, the hybrids showed reversible specific capacities up to ~330 mAh/g at 15 mA/g between 2 and 4.4 V vs. Li^+/Li. This improvement of electrochemical performance compared with pristine V_2O_5 is attributed to higher electric conductivity and enhanced bidimensionality.

References

[1] Sanchez, C., De, A. A., Soler-Illia, G. J., Ribot, F., Lalot, T., Mayer, C. R. and Cabuil, V. (2001). Chem. Mater., 13 , 3061–3083.
[2] Portier, J., Campet, G., Treuil, N., Poquet, A., Kim, Y. I., Kwon, S. J., Kwak, S. Y. and Choy, J. H. (1998). J. Korean Chem. Soc., 42, 487–500.
[3] Gangopadhyay, R. and De, A. (2000). Chem. Mater., 12, 608–622.
[4] Colvin, V. L., Schlamp, M. C. and Alivisatos, A. P. (1994). Nature (London), 370, 354.
[5] Leroux, F., Koene, B. E. and Nazar, L. F. (1996). J. Electrochem. Soc., 143, L181.
[6] Leroux, F., Goward, G., Power, W. P. and Nazar, L. F. (1997). J. Electrochem. Soc., 144, 3886.
[7] Goward, G. R., Leroux, F. and Nazar, L. F. (1998). Electrochim. Acta., 43, 1307.
[8] Wong, H. P., Dave, B. C., Leroux, F., Harreld, J., Dunn, B. and Nazar, L. F. (1998). J. Mater. Chem., 8, 1019.
[9] Harreld, J. H., Dunn, B. and Nazar, L. F. (1999). Int. J. Inorg. Mater., 1, 135.
[10] Lira-Cantu, M. and Gomez-Romero, P. (1999). Int. J. Inorg. Mater., 1, 111.
[11] Lira-Cantu, M. and Gomez-Romero, P. (1999). J. Electrochem. Soc., 146, 2029.
[12] Lira-Cantu, M. and Gomez-Romero, P. (1999). J. Solid State Chem., 147, 601.
[13] Kanatzidis, M. G. and Wu, C. U. (1989). J. Am. Chem. Soc., 111, 4141.

[14] Liu, Y. J., DeGroot, D. C., Schindler, J. L., Kannewurf, C. R. and Kanatzidis, M. G. (1993). J. Chem. Soc. Chem. Commun., 593.
[15] Wu, C. G., Degroot, D. C., Marcy, H. O., Schindler, J. L., Kannewurf, C. R., Liu, Y. J., Hirpo, W. and Kanatzidis, M. G. (1996). Chem. Mater., 8, 1992.
[16] Nalwa, H. S. (Ed.) (1997). Handbook of Organic Conductive Molecules and Polymers, Vols. 1–4. Wiley, Chichester, UK (for general reviews on conductive polymers).
[17] Groenedaal, L. B., Jonas, F., Freitag, F., Pielartzik, H. and Reynolds, J. R. (2000). Adv. Mater., 12, 481.
[18] Murugan, A. V., Kale, B. B., Kwon, C. W., Campet, G. and Vijayamohanan, K. (2001). J. Mater. Chem., 11, 2470.
[19] Murugan, A. V., Kwon, C. W., Campet, G., Kale, B. B., Maddanimath, T. and Vijayamohanan, K. (2002). J. Power Sources, 105, 1.
[20] Kwon, C. W., Murugan, A. V., Campet, G., Portier, J., Kale, B. B., Vijaymohanan, K. and Choy, J. H. (2002). Electrochem. Commun., 4, 384.
[21] Corradi, R. and Armes, S. P. (1997). Synth. Met., 84, 453.
[22] Aldebert, P., Baffier, N., Gharbi, N. and Livage, J. (1981). Mater. Res. Bull., 16, 669.
[23] Livage, J. (1996). Solid State Ionics, 935, 86–88.
[24] Warren, B. E. (1941). Phys. Rev., 59, 693.
[25] Sato, Y., Nomura, T., Tanaka, H. and Kobayakawa, K. (1991). J. Electrochem. Soc., 138, L37.
[26] Sato, Y., Asada, T., Tokugawa, H. and Kobayakawa, K. (1997). J. Power Sources, 68, 674.
[27] Sato, Y., Matsueda, T., Tokugawa, H. and Kobayawa, K. (1993). Chem. Lett., 901.
[28] Ugaji, M., Hibino, M. and Kudo, T. (1995). J. Electrochem. Soc., 142, 3664.
[29] Hibino, M., Ugaji, M., Kishimoto, A. and Kudo, T. (1995). Solid State Ionics, 79, 239.
[30] Gustafsson, J. C., Liedberg, B. and Inganas, O. (1994). Solid State Ionics, 69, 145.
[31] Kvarnstrom, C., Neugebauer, J., Blomquist, S., Ahonen, H. J., Kankare, J. and Ivaska, A. (1999). Electrochem. Acta., 44, 2739.
[32] Hernandez, V., Ramirez, F. J., Otero, T. F. and Lopez Navarrete, J. T. (1994). J. Chem. Phys., 100, 114.
[33] Aasmundtveit, K. E., Samuelson, E. J., Pettersson, L. A. A., Inganas, O., Johansson, T. and Feidenhans'l, R. (1999). Synth. Met., 101, 561.
[34] Aasmundtveit, K. E., Samuelson, E. J., Inganas, O., Pettersson, L. A. A., Johansson, T. and Ferrer, S. (2000). Synth. Met., 113, 93.
[35] Zotti, G., Zeechin, S., Schiavon, G. and Groenendaal, L. B. (2000). Chem. Mater., 12, 2996.
[36] Tran-Van, F., Garreau, S., Louarn, G., Froyer, G. and Chevrot, C. (2001). J. Mater. Chem., 11, 1378.
[37] Ross, R. A. and Fairbridge, C. (1984). Can. J. Chem., 62, 1483.
[38] Javadi, H. H., Cromack, K. R., McDiarmid, A. G. and Epstein, A. (1989). Phys. Rev. B, 39, 3579.
[39] Whittingham, M. S. (1998). In: Wakihara, M. and Yamamoto, O. (Eds.), Lithium Ion Batteries, Ch. 3. Kodansha, Tokyo.
[40] Le, D. B., Passerini, S., Tipton, A. L., Owens, B. B. and Smyrl, W. H. (1995). J. Electrochem. Soc., 142, L102.
[41] Le, D. B., Passerini, S., Guo, A. L. J., Ressler, J., Owens, B. B. and Smyrl, W. H. (1996). J. Electrochem. Soc., 143, 2099.
[42] Megahed, S., Barnett, B. M. and Xie, L. (Eds.) (1995). Rechargeable lithium and lithium ion batteries. In: Electrochemical Society Proceedings Series PV 94-28, Electrochemical Society, New Jersey.
[43] Lemmon, J. P. and Lerner, M. M. (1994). Chem. Mater., 6, 207.
[44] Oriakhi, C. O. and Lerner, M. M. (1996). Chem. Mater., 8, 2016.